Journal of Power Sources 189 (2009) 1292–1295

Contents lists available at ScienceDirect

Journal of Power Sources

journal homepage: www.elsevier.com/locate/jpowsour

Short communication

Electrochemically synthesized large area network of $Co_xNi_yAl_z$ layered triple hydroxides nanosheets: A high performance supercapacitor

Vinay Gupta [a,b,c,*], Shubhra Gupta [b], Norio Miura [b]

[a] Carbon Technology Unit, National Physical Laboratory, New Delhi 110012, India
[b] Art, Science and Technology Center for Cooperative Research, Kyushu University, Kasuga-shi, Fukuoka 816-8580, Japan
[c] Japan Science and Technology Agency, Kawaguchi-shi, Saitama 332-0012, Japan

ARTICLE INFO

Article history:
Received 21 November 2008
Received in revised form 5 January 2009
Accepted 15 January 2009
Available online 21 January 2009

Keywords:
$Co_xNi_yAl_z$
Layered triple hydroxides
Potentiostatic deposition
Specific capacitance
Supercapacitor

ABSTRACT

A network of $Co_xNi_yAl_z$ layered triple hydroxides (LTHs) nanosheets was prepared by the potentiostatic deposition process at −1.0 V (vs. Ag/AgCl) onto stainless steel electrodes. X-ray diffraction patterns show that the $Co_xNi_yAl_z$LTHs belong to the hexagonal system with layered structure. Cyclic voltammetry and charge discharge measurements in the potential range of −0.1 to 0.5 V and 0.0–0.4 V, respectively, vs. Ag/AgCl in 1 M KOH electrolyte indicate that $Co_xNi_yAl_z$LTHs have excellent supercapacitive characteristics. The maximum specific capacitance of ∼1263 F g^{-1} was obtained for $Co_{0.59}Ni_{0.21}Al_{0.20}$LTH. The impedance studies indicated highly conducting nature of the $Co_xNi_yAl_z$LTHs.

1. Introduction

Our increasing energy demands is at the crossroad, where soaring fuel prices, increasing pollution and depleting fuel reserve have forced us to search alternate power-energy sources. Electrochemical supercapacitors have higher energy density than dielectric capacitors and higher power density than batteries [1]. Owing to the unique energy storage performance, they have attracted considerable attention in many applications, e.g., hybrid electric vehicles, peak power sources, backup power storage, lightweight electronic fuses, starting power of fuel cells, memory protection of computer electronics, cellular devices, etc. [2–6].

Based on the different operation mechanisms, supercapacitors can be classified into two different categories: (1) double-layer capacitors, which are based on the non-Faradaic charge separation at the electrode/electrolyte interface, and (2) pseudocapacitors, which are based on the Faradaic redox reaction of electroactive materials. The materials studied for capacitor have been mainly of three types: carbon [7], metal oxide [8,9] and conducting polymer [10–12]. High-surface-area carbon materials (activated carbon black, carbon aerogel, and carbon nanotubes) are electrochemical double layer capacitors (EDLCs). Specific capacitance of up to ∼280 F g^{-1} could be achieved in the case of EDLCs [7]. Metal oxide and conducting polymer are pseudocapacitors. Initially, the hydrous ruthenium oxide was reported as the promising materials with specific capacitance value of 863 F g^{-1} [13]. However, due to its high cost, other metal oxides, such as manganese oxide [9], nickel oxide [14] and cobalt oxide [15] has been explored for supercapacitors.

Metal hydroxides are often layered materials with large interlayer spacing [16,17]. Recent development of metal hydroxides with high specific capacitances has regenerated great interest in such materials [18–25]. In the case of Co–Al LDHs, a maximum specific capacitance of 684 F g^{-1} was observed [19], whereas potentiostatically synthesized Co_xNi_{1-x}LDHs showed a maximum specific capacitance of 2104 F g^{-1}. $Co(OH)_2$/Y-zeolite composites showed a total specific capacitance of 1492 F g^{-1} [20] whereas in the case of $Co(OH)_2$–$Ni(OH)_2$/Y-zeolite composites, a specific capacitance of 479 F g^{-1} was obtained [22]. However, the characteristics of all these hydroxides suffered from asymmetric charge–discharge behavior. In this work, we have synthesized novel $Co_xNi_yAl_z$LTHs by potentiostatic deposition method. Their structural and capacitive characteristics showed that $Co_xNi_yAl_z$LTHs are very promising materials for supercapacitors.

2. Experimental

Analytical grade chemicals ($Co(NO_3)_2{\cdot}6H_2O$, $Ni(NO_3)_2{\cdot}6H_2O$, $Al(NO_3)_3{\cdot}9H_2O$ and 1 M KOH) and research grade stainless-steel

* Corresponding author at: Carbon Technology Unit, National Physical Laboratory, New Delhi 110012, India. Tel.: +91 9958144324; fax: +91 11 45609455.
E-mail address: drvinaygupta@netscape.net (V. Gupta).

0378-7753/$ – see front matter © 2009 Elsevier B.V. All rights reserved.
doi:10.1016/j.jpowsour.2009.01.026

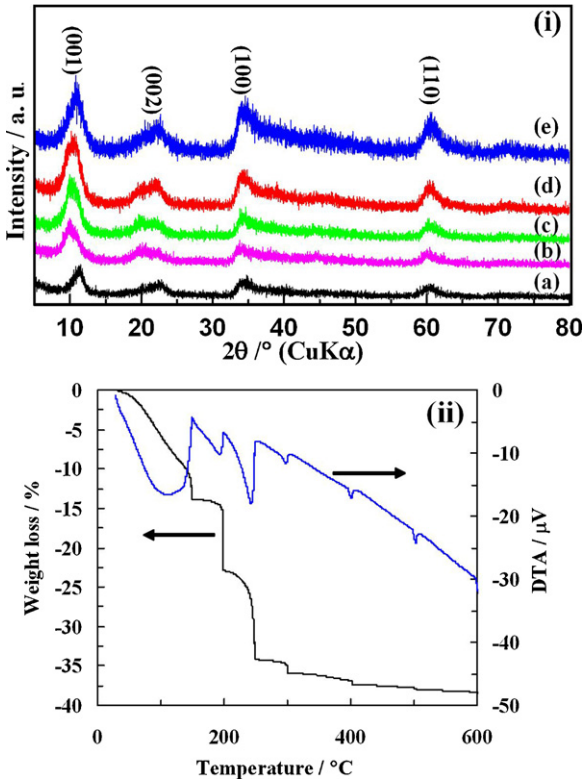

Fig. 1. (i) XRD patterns of the: (a) $Co_{0.75}Ni_{0.00}Al_{0.25}$LTHs, (b) $Co_{0.67}Ni_{0.13}Al_{0.20}$LTHs, (c) $Co_{0.59}Ni_{0.21}Al_{0.20}$LTHs, (d) $Co_{0.51}Ni_{0.29}Al_{0.20}$LTHs and (e) $Co_{0.31}Ni_{0.49}Al_{0.20}$LTHs and (ii) TG/DTA curves of the $Co_{0.59}Ni_{0.21}Al_{0.20}$LTHs.

Table 1
EDX analysis of Co, Ni and Al in $Co_xNi_yAl_z$LTHs.

Electrolyte solution Co:Ni:Al	Elemental composition $Co_xNi_yAl_z$LTHs[a]
0.90 M:0.00 M:0.10 M	$Co_{0.75}Ni_{0.00}Al_{0.25}$
0.75 M:0.25 M:0.10 M	$Co_{0.67}Ni_{0.13}Al_{0.20}$
0.60 M:0.40 M:0.10 M	$Co_{0.59}Ni_{0.21}Al_{0.20}$
0.50 M:0.50 M:0.10 M	$Co_{0.51}Ni_{0.29}Al_{0.20}$
0.25 M:0.75 M:0.10 M	$Co_{0.31}Ni_{0.49}Al_{0.20}$

[a] $x+y+z=1$.

(SS, grade 304, 0.2 mm thick) were used for $Co_xNi_yAl_z$LTHs preparations. The area of the SS for deposition was 3 cm × 4 cm. The SS was polished with emery paper to a rough finish, washed free of abrasive particles and then air-dried. An electrochemical cell was assembled in a three-electrode configuration in which the counter electrode was platinum (Pt), the reference electrode was Ag/AgCl (saturated KCl solution) and the working electrode was SS. The molar concentrations of the $Co(NO_3)_2{\cdot}6H_2O$:$Ni(NO_3)_2{\cdot}6H_2O$:$Al(NO_3)_3{\cdot}9H_2O$ aqueous solutions used for potentiostatic deposition were 0.25:0.75:10, 0.50:0.50:10, 0.60:0.40:10, 0.75:0.25:10 and 0.90:0.00:10. The potentiostatic deposition was carried out at the potential of −1.0 V vs. Ag/AgCl. The deposited electrodes were washed in distilled water by using a magnetic paddle in a beaker and then dried in an oven at 50 °C overnight. The weight of the deposit was measured by means of a micro-balance (Sartorius, BP211D) with an accuracy of 0.01 mg. The weights of all deposited $Co_xNi_yAl_z$LTHs were ~10 mg. The elemental analysis was carried out by use of an energy dispersive X-ray (EDX) spectrometer (EDAX, Horiba EX-220SE) coupled to a scanning electron microscope (Hitachi, S3000-N). The microstructure of the electrode materials was evaluated by use of a field emission scanning electron microscope (FE-SEM, JEOL, JSM-6340F). The X-ray diffraction patterns were obtained by use of an X-ray

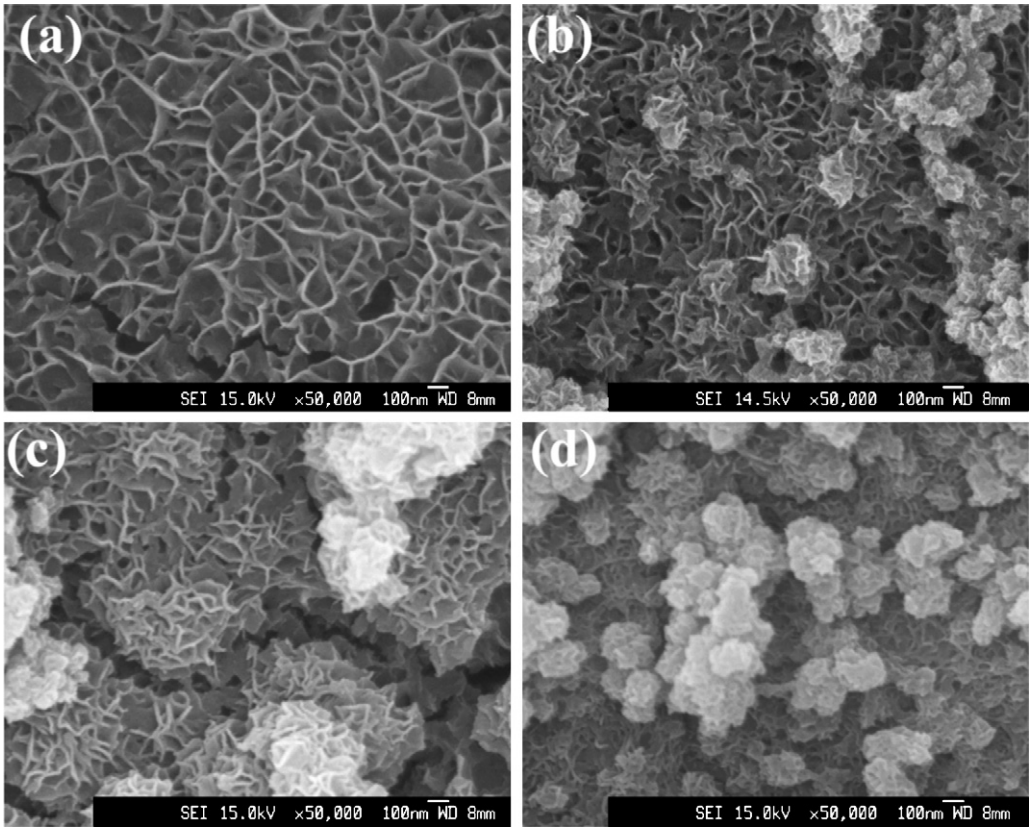

Fig. 2. SEM images of the $Co_xNi_yAl_z$LTHs: (a) $Co_{0.67}Ni_{0.13}Al_{0.20}$LTHs, (b) $Co_{0.59}Ni_{0.21}Al_{0.20}$LTHs, (c) $Co_{0.51}Ni_{0.29}Al_{0.20}$LTHs and (d) $Co_{0.31}Ni_{0.49}Al_{0.20}$LTHs.

diffractrometer (XRD, RIGAKU, R1NT2100) with Cu Kα radiation (λ = 1.5406 Å) operating at 40 kV, 20 mA. The TG/DTA curves were obtained by using an SII TG/DTA analyzer (Model 3200). All electrochemical depositions and capacitive measurements were performed by use of a potentiostat (AUTOLAB®, Eco Chemie, PGSTAT 30). The capacitive characterization was performed in 1 M KOH electrolyte.

3. Results and discussion

Table 1 shows the atomic percentages (at.%) of the elements Co, Ni and Al in $Co_xNi_yAl_z$ LTHs ($x+y+z=1$), obtained by means of EDX spectroscopy. The electrolyte concentration of $Al(NO_3)_3{\cdot}9H_2O$ was kept at 0.1 M in all the experiments. The elemental compositions of synthesized $Co_{0.75}Ni_{0.00}Al_{0.25}$LTHs, $Co_{0.67}Ni_{0.13}Al_{0.20}$LTHs, $Co_{0.59}Ni_{0.21}Al_{0.20}$LTHs, $Co_{0.51}Ni_{0.29}Al_{0.20}$LTHs and $Co_{0.31}Ni_{0.49}Al_{0.20}$LTHs were determined by EDX analysis. The compositions are arranged in increasing order of Ni content in Table 1.

Fig. 1(i) shows the XRD patterns of the Co_xNi_{1-x}LTHs. The patterns in Fig. 1(i) comprise four broad peaks appearing at 2θ values of 10.6° (7.75 Å), 21.4° (3.81 Å), 34.5° (2.68 Å) and 60.7° (1.55 Å) which correspond to α-$Co(OH)_2$, α-$Ni(OH)_2$ and α-$Al(OH)_3$. It was difficult to differentiate between the three phases, since they have similar structures, and their diffraction peaks are very close. Fig. 1(ii) shows the TG/DTA curves of the deposited $Co_{0.59}Ni_{0.21}Al_{0.20}$LTHs in 100 ml min^{-1} N_2 flow. The TG curve shows an initial weight loss of 5–6% at around 100 °C, which is due to the desorption of physically adsorbed water, and thereafter, the main weight loss of 19–20%, in the temperature range of 180–300 °C, may be due to the decomposition of the $Co_{0.59}Ni_{0.21}Al_{0.20}$LTH into the respective oxides, as shown in the inset of Fig. 1(ii). Since the loss of water of hydration occurs in the similar temperature range, its amount could not be estimated. The TG/DTA curves were similar for all of the deposits.

The SEM images of the deposited $Co_xNi_yAl_z$LTHs are shown in Fig. 2. As shown in Fig. 2a, a network of nano-thick $Co_{0.67}Ni_{0.13}Al_{0.20}$LTHs was observed. The microstructure becomes denser for the $Co_{0.59}Ni_{0.21}Al_{0.20}$LTH (Fig. 2b) and $Co_{0.51}Ni_{0.29}Al_{0.20}$LTHs (Fig. 2c). The densest structure is observed for the composition of $Co_{0.31}Ni_{0.49}Al_{0.20}$LTHs (Fig. 2d).

Fig. 3(i) shows the CV curves of the $Co_xNi_yAl_z$LTHs electrodes in 1 M KOH electrolyte at the scan rate of 10 mV s^{-1} in the potential range of −1.0 to +0.5 V. The $Co_xNi_yAl_z$LTHs electrodes showed very strong redox peaks due to the following Faradaic reactions of $Co(OH)_2$ and $Ni(OH)_2$ [23]:

$$Co(OH)_2 + OH^- \Leftrightarrow CoOOH + H_2O + e^- \quad (1)$$

$$CoOOH + OH^- \Leftrightarrow CoO_2 + H_2O + e^- \quad (2)$$

$$Ni(OH)_2 + OH^- \Leftrightarrow NiOOH + H_2O + e^- \quad (3)$$

The CV curves showed shifts in the redox peaks as the compositions of the $Co_xNi_yAl_z$LTHs electrodes were changed. It can be seen that the oxidation and reduction peaks for $Co_{0.75}Ni_{0.00}Al_{0.25}$ LTH are at 0.14 and 0.29 V, respectively. The oxidation peak is shifted to the higher potential and the reduction peak in most cases is shifted to the lower potential and become broad. For the composition of $Co_{0.31}Ni_{0.49}Al_{0.20}$LTH, the peaks are at 0.46 and 0.3 V for the oxidation and reduction processes, respectively. The redox area is highest for the $Co_{0.59}Ni_{0.21}Al_{0.20}$LTHs.

Fig. 3(ii) shows the charge–discharge (CD) curves of the $Co_xNi_yAl_z$LTHs electrodes in 1 M KOH electrolyte at 1 A g^{-1} current in the potential range between 0 and 0.4 V. The $Co_xNi_yAl_z$LTHs electrodes showed nearly ideal charge–discharge behavior. The specific capacitance values obtained from Fig. 3(ii) are shown in Fig. 4(i) where a specific capacitance value of 695 F g^{-1} was obtained for $Co_{0.75}Ni_{0.00}Al_{0.25}$LTHs. As the content of nickel is increased, an increase in the specific capacitance is observed. *The highest specific capacitance of* ∼1263 F g^{-1} *is obtained for* $Co_{0.59}Ni_{0.21}Al_{0.20}$*LTHs.* Incidentally, this is the highest specific capacitance obtained with nearly ideal charge–discharge characteristics conditions so far. A further increase in the Ni content decreases the specific capacitance to 1038 F g^{-1} for $Co_{0.51}Ni_{0.29}Al_{0.220}$LTHs. Liu et al. [25] have shown that in the case of $Co_xNi_yAl_z$LTHs prepared by precipitation method, a maximum specific capacitance value was 960 F g^{-1} can be obtained. Here we were able to obtain a much higher specific capacitance by potentiostatic deposition.

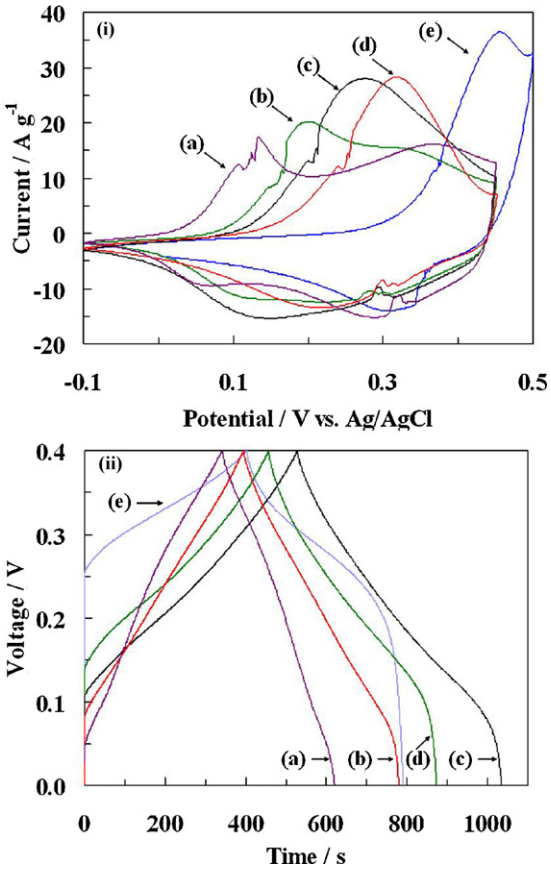

Fig. 3. (i) Cyclic voltammograms and (ii) charge–discharge curves of the: (a) $Co_{0.75}Ni_{0.00}Al_{0.25}$LTHs, (b) $Co_{0.67}Ni_{0.13}Al_{0.20}$LTHs, (c) $Co_{0.59}Ni_{0.21}Al_{0.20}$LTHs, (d) $Co_{0.51}Ni_{0.29}Al_{0.20}$LTHs and (e) $Co_{0.31}Ni_{0.49}Al_{0.20}$LTHs.

Fig. 4(ii) shows the electrochemical impedance spectra in the form of Nyquist plots for some $Co_xNi_yAl_z$LTHs electrodes at 0.4 V, where Z' and Z'' are the real and imaginary parts of the impedance, respectively. The plots obtained are composed of a semi-circle at high frequencies, which is related to Faradaic reactions. The slope close to 45° along the imaginary axis (Z'') at low frequencies is due to a Warburg impedance (a limiting diffusion process), and is not useful for charge storage. From the Nyquist plots, observed electrode resistances were close to 0.2 Ω. This shows that all the $Co_xNi_yAl_z$LTHs electrodes were of a highly conducting nature. The cyclic stability measurements of $Co_{0.59}Ni_{0.21}Al_{0.20}$LTHs at 5 A g^{-1} showed an initial specific capacitance loss of 10% in the first 500 cycles whereas it was 3% in the next 500 cycles which suggests that $Co_xNi_yAl_z$LTHs electrode tend to stabilize after the first 500 cycles. This capacitance loss initially might be due to some material loss which can be controlled by using a suitable membrane.

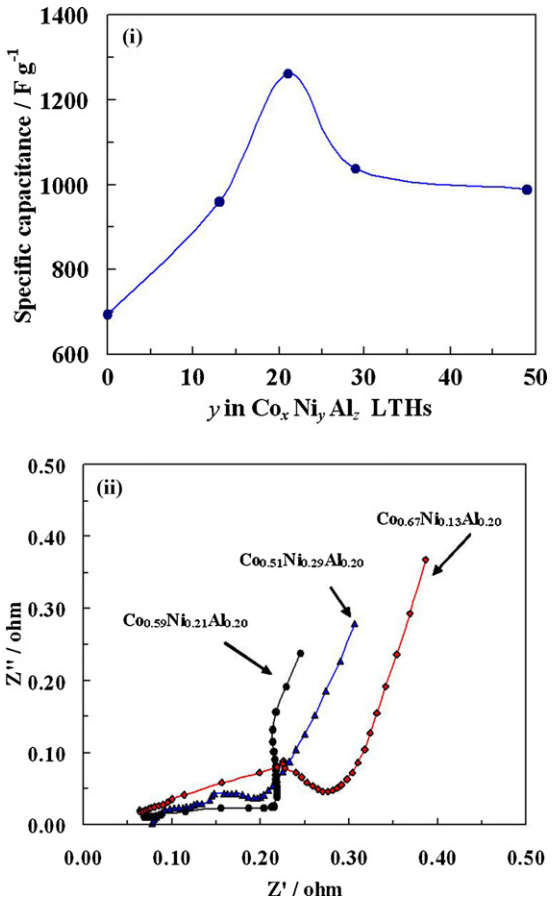

Fig. 4. (i) Specific capacitances of the $Co_xNi_yAl_z$LTHs as a function of y and (ii) Nyquist plots of $Co_xNi_yAl_z$LTHs with x values of 0.51, 0.59 and 0.67.

In conclusion, $Co_xNi_yAl_z$LTHs with anisotropic morphology were synthesized by the potentiostatic deposition method. Such morphology provided an accessible pathway for the intercalation of OH^- ions into the composite, as the interlayer space of the $Co_xNi_yAl_z$LTHs is compatible with the size of the hydrated ions (6–7.6 Å). The highest capacitance, ~1263 F g^{-1}, was observed for the $Co_{0.59}Ni_{0.21}Al_{0.20}$LTHs. The synthesized $Co_xNi_yAl_z$LTHs are very promising for supercapacitor application.

Acknowledgements

The present work was supported by the Japan Science and Technology (JST) Agency through the Core Research for Evolutionary Science and Technology (CREST) program under the project "Development of advanced nanostructured materials for energy conversion and storage".

References

[1] B.E. Conway, Electrochemical Supercapacitors, Kulwar Academic/Plenum Publishers, New York, 1999, p. 1.
[2] F. Beguin, K. Szostak, G. Lota, E. Frackowiak, Adv. Mater. 17 (2005) 2380.
[3] L.T. Lam, R. Louey, J. Power Sources 158 (2006) 1140.
[4] J.R. Miller, Electrochim. Acta 52 (2006) 1703.
[5] T.A. Centeno, F. Stoeckli, in: V. Gupta (Ed.), Recent Advances in Supercapacitors, Transworld Research Network, Kerala, India, 2006, p. 57.
[6] J.R. Miller, A.F. Burke, Interface 17 (2008) 53.
[7] P. Simon, A.F. Burke, Interface 17 (2008) 38.
[8] D. Bélanger, T. Brousse, J.W. Long, Interface 17 (2008) 49.
[9] T. Shinomiya, V. Gupta, N. Miura, Electrochem. Acta 51 (2006) 4412.
[10] D.J.P. Zheng, P.J. Cygan, T.R. Jow, J. Electrochem. Soc. 142 (1995) 2699.
[11] V. Gupta, N. Miura, Electrochem. Solid State Lett. 8 (2005) A630–A632.
[12] V. Gupta, N. Miura, J. Power Sources 157 (2006).
[13] D.J.H. Jang, K. Machida, Y. Kim, K. Naoi, Electrochem. Acta 52 (2006) 1733.
[14] K.W. Nam, K.W. Kim, J. Electrochem. Soc. 149 (2002) A346.
[15] V. Srinivasan, J.W. Weidner, J. Power Sources 108 (2002) 15.
[16] R.S. Jayashree, P.V. Kamath, J. Mater. Chem. 9 (1999) 961.
[17] T.N. Ramesh, M. Rajamathi, P.V. Kamath, Solid State Ionics 5 (2003) 751.
[18] D.D. Zhao, S.S. Bao, W.J. Zhou, H.L. Li, Electrochem. Commun. 9 (2007) 869.
[19] Y. Wang, W. Yang, S. Zhang, D.G. Evans, X. Duan, J. Electrochem. Soc. 152 (2005) A2130.
[20] V. Gupta, S. Gupta, N. Miura, J. Power Sources 175 (2008) 680.
[21] J.H. Park, O.O. Park, K.H. Shin, C.S. Jin, J.H. Kim, Electrochem. Solid State Lett. 5 (2002) H7.
[22] L. Cao, F. Xu, Y.Y. Liang, H.L. Li, Adv. Mater. 16 (2004) 1853.
[23] Y.Y. Liang, S.J. Bao, H.L. Li, J. Solid State Electrochem. 11 (2007) 571.
[24] C.C. Hu, C.Y. Cheng, Electrochem. Solid State Lett. 5 (2002) A43.
[25] X.M. Liu, Y.H. Zhang, X.G. Zhang, S.Y. Fu, Electrochem. Acta 49 (2004) 3141.